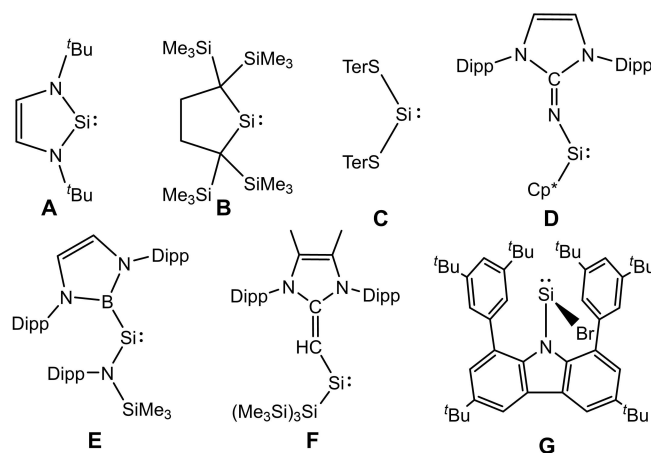




# Silylenes with a Small Chalcogenide Substituent: Tuning Frontier Orbital Energies from O to Te

Maximilian P. Müller and Alexander Hinz\*

**Abstract:** The general synthesis of heteroleptic acyclic silylenes with a bulky carbazolyl substituent (<sup>dtbp</sup>Cbz) is detailed and a series of compounds with a chalcogenide substituent of the type [(<sup>dtbp</sup>Cbz)SiE<sup>16</sup>R] (E<sup>16</sup>R = O<sup>t</sup>Bu, SEt, SePh, TePh) is reported. With the bulky carbazolyl substituent present, the chalcogenide moiety can be very small, as is shown by incorporating groups as small as ethyl, phenyl or *tert*-butyl. For the first time, the electronic properties of the silylene can be tuned along a complete series of chalcogenide substituents. The effects are clearly visible in the NMR and UV/Vis spectra, and were rationalised by DFT computations. The reactivity of the heaviest chalcogenide-substituted silylenes was probed by reactions with trimethylphosphine selenide and the terphenyl azide TerN<sub>3</sub> (Ter = 2,6-dimesitylphenyl).



Scheme 1. Selected known silylenes.

## Introduction

Divalent silicon compounds have attracted great interest since Jutzis's discovery of silococene in 1986.<sup>[1]</sup> While this example features divalent silicon, it is not a typical silylene because of the unique properties of Cp ligands. Utilising the same strategy that had helped to stabilise carbenes before by Arduengo,<sup>[2]</sup> Denk et al. prepared the first genuine silylene in 1994 (Scheme 1, **A**).<sup>[3]</sup> The involvement of N-substituents contributed to the stabilisation, but also diminished the acidity of the silylene. Five years later, Kira obtained a cyclic dialkyl silylene with higher reactivity (**B**).<sup>[4]</sup> In 2006, Driess obtained cyclic dicoordinated silylenes derived from the  $\beta$ -diketiminato scaffold.<sup>[5,6]</sup> Reversible base-stabilisation of silylenes was discovered by Tokitoh and Okazaki who trapped a diarylsilylene with an isonitrile.<sup>[7,8]</sup> Later, Roesky and Filippou employed carbenes as stronger bases to obtain adducts of divalent silicon halides, NHC-SiX<sub>2</sub> (NHC = N-heterocyclic carbene)<sup>[9,10]</sup> where in subse-

quent reactions the NHC can either be retained or dissociated.<sup>[11–15]</sup> The concept of base-stabilisation was also employed successfully in Roesky's amidinosilylene,<sup>[16]</sup> Kato's phosphine-amido silylenes<sup>[17,18]</sup> and Nakata's imidophosphonamidossilylene<sup>[19]</sup> which feature bidentate monoanionic ligands and enabled rich chemistry. Acyclic silylenes proved to be a synthetic challenge that was solved simultaneously by Power (**C**), Inoue (**D**) and Aldridge (**E**). While Power employed bulky terphenylthiolato substituents (**C**) in his work,<sup>[20]</sup> Inoue introduced an N-heterocyclic imino scaffold (NHI) to silylene chemistry and prepared (NHI)SiCp\* (**D**).<sup>[21]</sup> Aldridge initially reported on the borylsilylene **E** and subsequently developed a modular access to borylsilylenes with a bulky silyl substituent.<sup>[22,23]</sup> Other acyclic silylenes were since then developed by Inoue, employing NHI and a bulky silyl substituents.<sup>[24–27]</sup> These silylenes reversibly form silepins and the equilibrium was observed spectroscopically.<sup>[28]</sup> Rivard incorporated the related N-heterocyclic olefin substituents (NHO) in a bis-NHO silylene and NHO/silyl silylene (**F**) where he did not observe silepin formation.<sup>[29,30]</sup> Inoue recently demonstrated, that backbone methylation of NHI substituents also inhibits silepin formation in that case.<sup>[31]</sup> In another line of investigation, Aldridge introduced a boryloxy substituent, isoelectronic to NHI as well, and prepared the corresponding bis-substituted silylene.<sup>[32]</sup> In all these instances, two bulky substituents are required.

We have reported on the first acyclic halosilylenes [(<sup>dtbp</sup>Cbz)SiBr] (<sup>dtbp</sup>Cbz = 1,8-bis(3,5-di-*tert*-butylphenyl)-3,6-di-*tert*-butyl-carbazolyl, **G**) and [(<sup>dtbp</sup>Cbz)SiI] in 2020, where the bulky carbazolyl substituent <sup>dtbp</sup>Cbz was incorporated.<sup>[33]</sup>

[\*] M. Sc. M. P. Müller, Dr. A. Hinz  
 Karlsruhe Institute of Technology (KIT)  
 Institute for Inorganic Chemistry (AOC)  
 Engesserstr. 15, 76131 Karlsruhe  
 E-mail: alexander.hinz@kit.edu

© 2024 The Authors. Angewandte Chemie International Edition published by Wiley-VCH GmbH. This is an open access article under the terms of the Creative Commons Attribution License, which permits use, distribution and reproduction in any medium, provided the original work is properly cited.

Recently, Guthardt and Jones prepared a boryloxy substituent and a derived dicoordinated bromosilylene.<sup>[34]</sup>

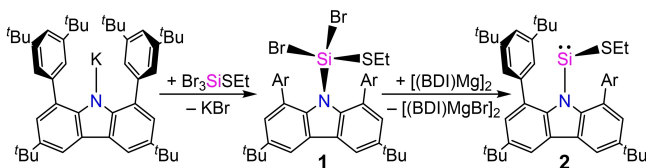
In this contribution, we show that steric bulk on chalcogenide substituents of acyclic dicoordinated silylenes is not required by establishing the series of compounds [(<sup>dtbp</sup>Cbz)SiE<sup>16</sup>R] (E<sup>16</sup>R = O<sup>t</sup>Bu, SEt, SePh, TePh) to allow fine tuning of the silylene frontier orbital energies.

## Results and Discussion

The most obvious way of generating new acyclic silylenes after obtaining the bromosilylene [(<sup>dtbp</sup>Cbz)SiBr] is salt metathesis with any other metalated nucleophile R–M, in analogy to methods frequently used with Roesky's amidinato chlorosilylene.<sup>[35–39]</sup> Unfortunately, with the carbazolyl substituent these metathesis reactions generally do not work as intended, because the alkali metal complexes [(<sup>dtbp</sup>Cbz)M] are formed as major product.<sup>[40]</sup> Consequently, other methods had to be explored. As we have previously attempted to introduce thiolato substituents to silanes,<sup>[41]</sup> the thiolatosilylene was our first target. A good reagent to transfer ethyl thiolato groups is Pb(SEt)<sub>2</sub><sup>[42]</sup> and when SiBr<sub>4</sub> was treated with Pb(SEt)<sub>2</sub>, Br<sub>3</sub>SiSEt could be isolated as a pure colourless liquid in accord with literature reports.<sup>[43]</sup> Subsequent metathesis with [(<sup>dtbp</sup>Cbz)K] resulted in the formation of [(<sup>dtbp</sup>Cbz)SiBr<sub>2</sub>SEt] (**1**, Scheme 2). This thiolatosilane could be reduced with the Mg(I) compound [(<sup>Mes</sup>BDI)Mg]<sub>2</sub> (BDI = β-diketiminato, Mes = mesityl)<sup>[44]</sup> which had worked best in the bromosilylene synthesis as well,<sup>[33]</sup> and afforded the thiolatosilylene [(<sup>dtbp</sup>Cbz)SiSEt] (**2**).

The reduction reaction can be followed straightforwardly by NMR spectroscopy. Characteristic resonances of the ethyl group of **1** in the <sup>1</sup>H NMR spectrum at 0.66 and 1.95 ppm are downfield-shifted to 0.78 and 2.14 ppm in **2**. Similarly, the carbazolyl C<sup>4,5</sup>H signals are observed at lower field in **2** (**1**: 8.17 ppm, **2**: 8.49 ppm). The most striking effect was observed in the <sup>29</sup>Si NMR spectrum, where the signal of **1** at –23.9 ppm in the typical silane region disappears, and instead a resonance at +205.6 ppm was found which is more shielded than that of Power's bithiolatosilylene **C** (+285.5 ppm).<sup>[20]</sup> The only resonance that is upfield-shifted upon reduction is the <sup>13</sup>C NMR signal of the α-C atom of the ethyl group, which was found at 26.13 ppm in **1** and at 24.23 ppm in **2**, while the β-C atom was observed at 15.83 ppm in **1** and at 18.73 ppm in **2**.

Structurally, thiolatosilylene **2** displays a Si–S distance of 2.1193(9) Å, a S–C distance of 1.864(3) Å and a Si–N distance of 1.810(2) Å as well as near orthogonal C–S–Si



**Scheme 2.** Synthesis of ethylthiolatosilylene **2** (Ar = 3,5-di-*tert*-butylphenyl).

and S–Si–N angles of 95.60(11)° and N1–Si1–S1 96.48(6)°, respectively (Figure 1). All bonds are elongated compared to those in the silane precursor **1** (Si–C1 1.812(3), Si–Si1 2.0961(9), Si1–N1 1.752(2) Å) and the angle at the Si atom is considerably more acute (**1**: N1–Si1–S1 118.11(7)°).

For the alkoxides, it was not feasible to isolate mono-substituted tribromosilanes Br<sub>3</sub>SiOR (R = Et, Mes). However, <sup>t</sup>BuOSiBr<sub>3</sub> could be obtained by treatment of SiBr<sub>4</sub> with KO<sup>t</sup>Bu. This, in turn, did not allow access to [(<sup>dtbp</sup>Cbz)SiBr<sub>2</sub>O<sup>t</sup>Bu] (**3**) by metathesis with [(<sup>dtbp</sup>Cbz)K], as only decomposition was observed. We turned again to attempts of metathesis at <sup>dtbp</sup>CbzSiBr<sub>3</sub> which eventually succeeded when KO<sup>t</sup>Bu was employed (Scheme 3), affording [(<sup>dtbp</sup>Cbz)SiBr<sub>2</sub>O<sup>t</sup>Bu] (**3**). Treatment with [(<sup>Mes</sup>BDI)Mg]<sub>2</sub> enabled the formation of the corresponding silylene [(<sup>dtbp</sup>Cbz)SiO<sup>t</sup>Bu] (**4**) but required heating to 105 °C overnight for complete consumption of the reducing agent.

Upon reduction, the <sup>29</sup>Si NMR resonance of **3** at –70.2 ppm disappeared and instead, **4** was observed at +96.3 ppm, more downfield-shifted than that of Inoue's (NHI)SiOSi<sup>t</sup>Bu<sub>3</sub> (+58.9 ppm).<sup>[26]</sup> Also, in this instance, the α-C atom becomes more shielded after reduction (**3**: 80.35 ppm, **4**: 74.64 ppm). The molecular structure of **4** (Figure 2, Si–O1 1.6354(8), Si1–N1 1.8257(9), O1–C49 1.458(2) Å) shows longer Si–O, O–C and

Si–N distances than that of **3** (Si–O1 1.595(2), Si1–N1 1.741(2), O1–C49 1.453(3), Å) as well as more acute

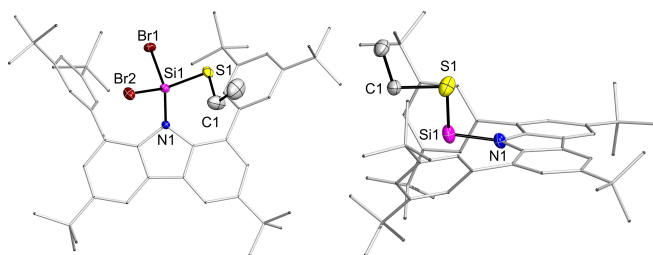
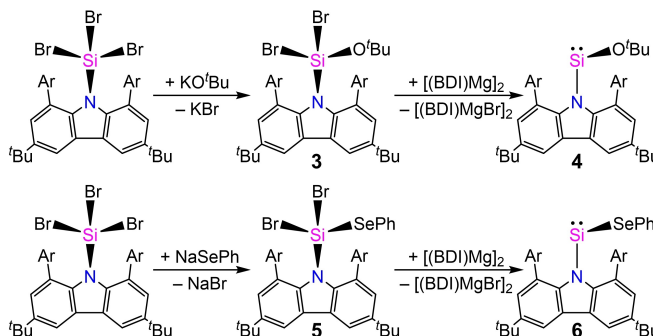


**Figure 1.** Molecular structure of **1** and **2** with thermal ellipsoids depicted at 50% probability. Selected bond lengths [Å] and angles [°] for **1**: Si–C1 1.812(3), Si–Si1 2.0961(9), Si1–N1 1.7523(2), C1–Si1–Si1 103.55(11), N1–Si1–S1 118.11(7). For **2**: Si–C1 1.864(3), Si–Si1 2.1193(9), Si1–N1 1.810(2), C1–Si1–Si1 95.60(11), N1–Si1–S1 96.48(6).



**Scheme 3.** Synthesis of alkoxy-silylene **4** and selenolato-silylene **6** (Ar = 3,5-di-*tert*-butylphenyl).

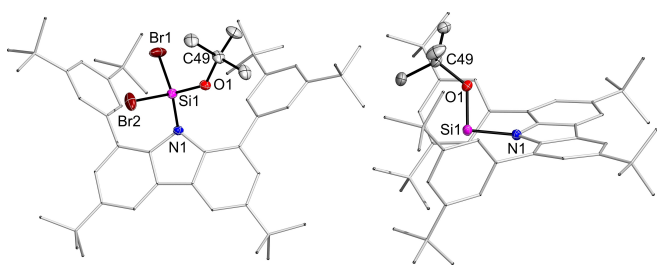


**Figure 2.** Molecular structure of **3** and **4** with thermal ellipsoids depicted at 50% probability. Selected bond lengths [Å] and angles [°] for **3**: Si1–O1 1.595(2), Si1–N1 1.741(2), O1–C49 1.453(3), O1–Si1–N1 108.74(11), C49–O1–Si1 137.34(19). For **4**: Si1–O1 1.6354(8), Si1–N1 1.8257(9), O1–C49 1.458(2), O1–Si1–N1 95.84(4), C49–O1–Si1 128.74(7).

O–Si–N and C–O–Si angles (**3**: O1–Si1–N1 108.74(11), C49–O1–Si1 137.3(2), **4**: O1–Si1–N1 95.84(4), C49–O1–Si1 128.74(7)°).

Very similar to the alkoxy-silylene, synthetic access to the selenolatosilylene could be found. The silane [(<sup>dtbp</sup>Cbz)SiBr<sub>2</sub>] was found to cleanly react with NaSePh in a mixture of toluene and DME to yield [(<sup>dtbp</sup>Cbz)SiBr<sub>2</sub>SePh] (**5**, Scheme 3). This could be reduced by [(<sup>Mes</sup>BDI)Mg]<sub>2</sub> at slightly elevated temperature (45 °C, overnight), affording [(<sup>dtbp</sup>Cbz)SiSePh] (**6**) as pale yellow solid. The <sup>29</sup>Si NMR

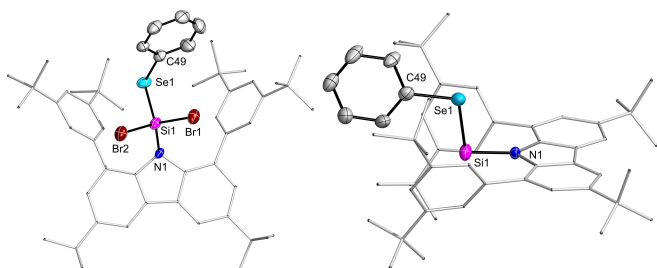
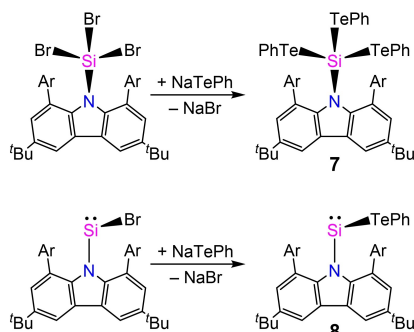


**Figure 3.** Molecular structure of **5** and **6** with thermal ellipsoids depicted at 50% probability. Selected bond lengths [Å] and angles [°] for **5**: Se1–C49 1.926(8), Se1–Si1 2.244(3), Si1–N1 1.747(6), C49–Se1–Si1 95.9(3), N1–Si1–Se1 111.2(2). For **6**: Se1–C49 1.914(3), Se1–Si1 2.2976(9), Si1–N1 1.820(2), C49–Se1–Si1 100.19(9), N1–Si1–Se1 94.61(7).



**Scheme 4.** Synthesis of tellurolatosilane **7** and tellurolatosilylene **8** (Ar = 3,5-di-*tert*-butylphenyl).

spectrum of **5** shifts from –32.0 ppm to 213.4 ppm in **6**, with a marginally increased <sup>1</sup>J<sub>SiSe</sub> coupling constant from 204 to 229 Hz. In the same way, the <sup>77</sup>Se NMR signal shifts from 227.0 to 612.4 ppm.

Structurally, **5** and **6** show a smaller increase of bond lengths upon reduction compared to **2** and **4** (Figure 3, **5**: Se1–C49 1.926(8), Se1–Si1 2.244(3), Si1–N1 1.747(6), **6**: Se1–C49 1.914(3), Se1–Si1 2.2976(9), Si1–N1 1.820(2) Å). The difference in the angles is also smaller, while the tendency remains (**5**: C49–Se1–Si1 95.9(3), N1–Si1–Se1 111.2(2), **6**: C49–Se1–Si1 100.19(9), N1–Si1–Se1 94.61(7)°).

When an analogous protocol was applied targeting the tellurolatosilane [(<sup>dtbp</sup>Cbz)SiBr<sub>2</sub>TePh], instead the trisubstituted [(<sup>dtbp</sup>Cbz)Si(TePh)<sub>3</sub>] (**7**, Scheme 4) was obtained. This could not be reduced productively, and again other routes had to be explored. Fortunately, in this instance, the direct metathesis of bromosilylene [(<sup>dtbp</sup>Cbz)SiBr] with NaTePh was possible and afforded the desired tellurolatosilylene [(<sup>dtbp</sup>Cbz)SiTePh] (**8**). Spectroscopically, the silane **7** features a resonance at –48.0 ppm in the <sup>29</sup>Si NMR spectrum with satellites due to <sup>1</sup>J<sub>SiTe</sub> coupling of 521 Hz. The corresponding resonance in the <sup>125</sup>Te NMR spectrum is broadened and was observed at 275 ppm. In contrast, for the silylene **8**, both are downfield-shifted, so that the resonances are observed at 246.7 ppm in the <sup>29</sup>Si NMR spectrum and at 806.2 ppm in the <sup>125</sup>Te NMR spectrum with a <sup>1</sup>J<sub>SiTe</sub> coupling constant of 536 Hz. Compared to the Si(IV) compound **7** (Figure 4), in **8** the N–Si, Si–Te and Te–C bonds are only marginally elongated (**7**: Te1–C1 2.135(4), Te1–Si1 2.5190(11), Si1–N1 1.808(3), **8**: Te1–C49 2.132(4), Te1–Si1 2.531(2), Si1–N1 1.820(3) Å).

With a complete series of chalcogenide-substituted acyclic silylenes available, a comparative computationally supported analysis can be undertaken. The calculations were carried out with Gaussian16 with the PBE0 functional and def2-TZVP basis sets. The structural parameters show Si–E bond lengths that deviate considerably from the sum of covalent radii for the lighter chalcogens (Table 1).<sup>[45]</sup> The polarisation of the Si–E bond decreases from O to Te as the difference in electronegativity decreases. The charge on Si decreases as well from +1.35 for **4** (O<sup>t</sup>Bu) to +0.79 for **8**

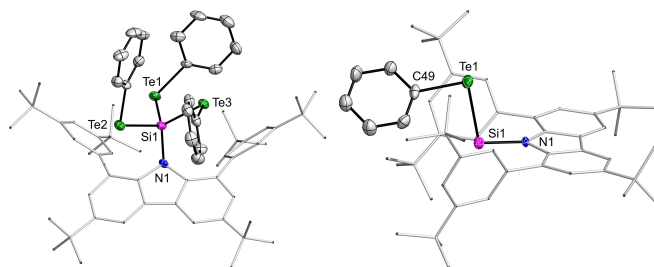


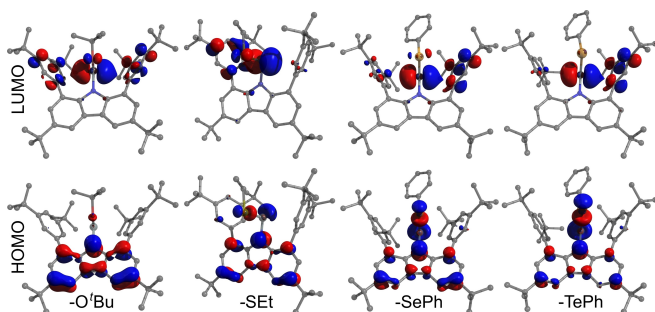
**Figure 4.** Molecular structure of **7** and **8** with thermal ellipsoids depicted at 50% probability. Selected bond lengths [Å] and angles [°] for **7**: Te1–C1 2.135(4), Te1–Si1 2.5190(11), Si1–N1 1.808(3), C1–Te1–Si1 97.28(11), N1–Si1–Te1 108.83(11). For **8**: Te1–C49 2.132(4), Te1–Si1 2.531(2), Si1–N1 1.820(3), C49–Te1–Si1 91.7(2), N1–Si1–Te1 99.52(11).

**Table 1:** XRD structural data for chalcogenide-substituted silylenes [(<sup>dtb</sup>pCbz)SiE<sup>16</sup>R].

compound	4	2	6	8
E <sup>16</sup> R	O <sup>t</sup> Bu	SEt	SePh	TePh
Si–E	1.6354(8)	2.1193(9)	2.2976(9)	2.531(2)
Σr <sub>cov</sub> <sup>[45]</sup>	1.79	2.19	2.32	2.52
Si–N	1.8257(9)	1.801(2)	1.820(2)	1.820(3)
N–Si–E	95.84(4)	96.48(6)	94.61(7)	99.52(11)
Si–E–C	128.74(7)	95.60(11)	100.19(9)	91.7(2)

(TePh). Consequently, the Wiberg bond index is only 0.51 for **4** (O<sup>t</sup>Bu) and increases to 1.07 for **8** (TePh).

The frontier orbitals of the four silylenes are depicted in Figure 5. The LUMO is generally dominated by the unoccupied p atomic orbital of the Si atom. Its energy progressively decreases from –1.125 to –1.617 eV the

**Figure 5.** Frontier orbitals of **4**, **2**, **6** and **8**.**Table 2:** Spectroscopic and computational data of chalcogenide-substituted silylenes [(<sup>dtb</sup>pCbz)SiE<sup>16</sup>R] (δ in ppm, λ<sub>max</sub> in nm, E in eV, q and orbital occupations in e).<sup>[a]</sup>

compound	4	2	6	8
E <sup>16</sup> R=	O <sup>t</sup> Bu	SEt	SePh	TePh
obs. δ( <sup>29</sup> Si)	96.3	205.6	213.4	246.7
λ <sub>max</sub> (obs.)	358	408	436	484
λ <sub>max</sub> (comp.)	367	419	433	464
E(LUMO)	–1.125	–1.427	–1.520	–1.617
E(HOMO)	–5.396	–5.327	–5.309	–5.233
NBO analysis <sup>[b]</sup>				
q(Si)	1.35	0.97	0.91	0.79
q(E)	–0.99	–0.30	–0.11	0.08
WBI(Si–E)	0.51	0.94	0.98	1.07
Si(LP)	1.92	1.95	1.92	1.92
E(LP1) <sup>[c]</sup>	1.95	1.97	1.96	1.97
E(LP2) <sup>[d]</sup>	1.86	1.79	1.76	1.75
bond (Si–E)	1.98	1.91	1.86	1.80
Si(LP*)	0.24	0.26	0.35	0.36
composition of Si–E	0.07/0.93 <sup>[b]</sup>	0.19/0.81	0.21/0.79	0.24/0.76
AIM analysis <sup>[47]</sup>				
ρ	0.116	0.091	0.084	0.076
∇ <sup>2</sup> (ρ)	0.885	0.135	0.029	–0.10
N (ELF) <sup>[48]</sup>	0.10	0.29	0.41	0.82

[a] Gaussian16/PBE0/Def2-SVP/GD3BJ. [b] By default, the N–Si bond is ionic in the NBO picture, as is the Si–O bond. [c] dominant s-type AO. [d] dominant p-type AO.

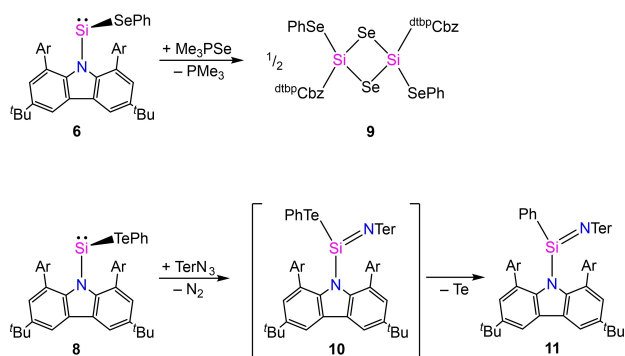
heavier the chalcogen is (see Table 2). The HOMO shows contributions from the carbazole π scaffold. The contribution of a σ(Si–E) bonding orbital as well as an s-type Si atomic orbital increases the heavier the chalcogen is (Figure 5). However, the change in HOMO energy is smaller and increases from –5.396 eV for **4** (O<sup>t</sup>Bu) to –5.233 eV for **8** (TePh). It should be noted that the transition from alkyl to aryl substituents along the series of silylenes also impacts the frontier orbital energies: For **6** and **8**, the HOMO and LUMO energies are 0.07 and 0.02 eV higher than for their ethyl-substituted analogues. The combined effects on the frontier orbitals are detectable in the lowest-energy electronic transition, which is shifted from 358 nm for the alkoxy-substituted silylene **4** to 484 nm for the tellurolatosilylene **8**.

Spectroscopically, it is also interesting to note that upon formation of silylene from silane precursors, many characteristic resonances in the <sup>1</sup>H, <sup>13</sup>C, <sup>29</sup>Si, <sup>77</sup>Se and <sup>125</sup>Te NMR spectra are downfield-shifted, with the exception of the α-C of the chalcogenide substituent. This effect is reproduced for the alkoxy and thiolato substituents by DFT calculations (see Supporting Information 4.1).

NBO analysis was conducted to gain further insight into the electronic structure. For all four silylenes, there are s-type natural valence orbitals at both silicon and the chalcogen which show a near-integer occupation > 1.9 e. In contrast, the p-type non-bonding orbital of the chalcogen shows decreased occupation between 1.86 for **4** (O<sup>t</sup>Bu) and 1.75 for **8** (TePh), indicating a degree of delocalisation towards the Si atom. This is reflected by occupation of the p-type natural orbital at silicon which increases from 0.24 with the O<sup>t</sup>Bu substituent to 0.36 for the TePh group. The nature of the Si–E bond changes as well with increasing atomic number of E. Corresponding with the electronegativity difference, natural charges and bond polarisation decrease, while the Wiberg bond index increases as the bond is more and more covalent. An AIM analysis<sup>[46,47]</sup> also shows drastic change of the Si–E bond from O to Te: For the alkoxy-silylene, the bond critical point shows a depletion of electron density and a positive ∇<sup>2</sup>(ρ) which, in conjunction with a small ELF basin population N,<sup>[48]</sup> is indicative of charge-shift bonding.<sup>[49,50]</sup> These factors are diminished but still present for the heavier homologues, until Te, where the Si–Te bond resembles a conventional covalent bond with ∇<sup>2</sup>(ρ) > 0 and the occupation of the ELF basin close to 1.

The reactivity of the selenolato-substituted silylene **6** was probed by oxidation with trimethylphosphine selenide which yielded the dimerisation product [(<sup>dtb</sup>pCbzSi(SePh)(μ-Se))<sub>2</sub> (**9**, Scheme 5). The product was crystallised and structurally characterised, but proved insoluble in all common organic solvents afterwards, so no solution-phase characterisation can be provided. Similar dimerisations have been observed for silanones derived from dicoordinated silylenes.<sup>[51–53]</sup>

The structure of **9** features a central Si<sub>2</sub>Se<sub>2</sub> core (Figure 6) with two nearly identical Si–Se contacts (2.2744(7), 2.2810(7) Å) as well as a slightly contracted exocyclic Si–Se bond of 2.2517(7) Å. These values compare well with the ones observed in **5** and **6**.



**Scheme 5.** Reactivity of **6** towards  $\text{Me}_3\text{PSe}$  and of **8** towards  $\text{TerN}_3$  (Ar = 3,5-di-*tert*-butylphenyl, Ter = 2,6-dimesitylphenyl).

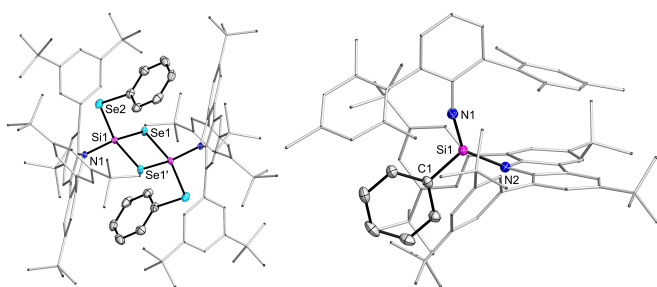


**Figure 6.** Molecular structure of **9** and **11** with thermal ellipsoids depicted at 50% probability. Selected bond lengths [Å] and angles [°] for **9**: Se1–Si1 2.2744(7), Se1–Si1 2.2810(7), Se2–C49 1.917(3), Se2–Si1 2.2517(7), Si1–N1 1.772(2), Si1–Se1–Si1' 82.91(3). For **11**: Si1–N1 1.5526(14), Si1–N2 1.752(2), Si1–C1 1.835(2), N1–C7 1.379(2), N1–Si1–N2 129.51(7), N1–Si1–C1 119.02(7), N2–Si1–C1 111.45(7).

The behaviour of tellurolo-substituted silylene **8** was probed by reaction with the terphenyl azide  $\text{TerN}_3$  (Scheme 5, Ter = 2,6-dimesitylphenyl). The putative initial reaction product **10** was not stable and decomposed within hours. It could, however, be characterised by NMR spectroscopy as it shows a broad  $^{29}\text{Si}$  resonance at  $-41$  ppm and a corresponding broad  $^{125}\text{Te}$  NMR resonance at  $146$  ppm. As the decomposition proceeded and tellurium deposited, the iminosilane [ $^{\text{dtbp}}\text{CzbzSi}(\text{Ph})=\text{N}(\text{Ter})$ ] **11** was formed as major product. The elimination of Te transformed the TePh group into a Ph moiety. In the reaction mixture, **11** was characterised by  $^{29}\text{Si}$  NMR spectroscopy with a sharp resonance at  $-38.7$  ppm.

Crystalline material of the compound was eventually obtained and the product was identified by SC-XRD experiments (Figure 6). It is noteworthy, that iminosilane **11** is stable, while silaimidoylbromide with Br instead of Ph was not obtained.<sup>[54]</sup> Structurally, the iminosilane **11** features a planarised Si atom (sum of angles  $360^\circ$ ) and a short Si=N double bond of  $1.553(2)$  Å, comparing well to other iminosilanes ( $1.549$ – $1.573$  Å).<sup>[55,56]</sup>

## Conclusion

We have shown that for acyclic silylenes with chalcogenide substituents, steric bulk is not required on that part of the molecule. The synthesis is not straightforward and follows a metathesis and reduction approach. For the thiolatosilylene, the introduction of the chalcogenide moiety was required prior to carbazoyl substitution, while for the alkoxide and selenolato substituent the chalcogenide was incorporated at the stage of carbazoylsilane. In contrast, the tellurolo-silylene could only be prepared by direct metathesis with the carbazoylbromosilylene. Thus, a complete series with small substituents spanning the whole series of chalcogens was investigated, allowing the fine tuning of electronic properties of the silylene. The bonding situation was elucidated by computational methods, revealing that the changes in bond polarity and covalency directly impact the silicon atom, which is then reflected in observable properties such as UV/Vis and NMR spectra. The heavier the chalcogen is, the smaller is the HOMO–LUMO gap, and the more deshielded the  $^{29}\text{Si}$  nucleus becomes. An initial reactivity test showed that in particular for the Te-based substituent, the heavy chalcogenide can be expelled from the product, so that the substituent is transferred directly onto silicon, due to the inherent weakness of the Si–Te bond. Further studies to expand the scope of substituents on carbazoyl silylenes are in progress.

## Supporting Information

The authors have cited additional references within the Supporting Information.<sup>[57–74]</sup>

Deposition Numbers 2335645 (**1**), 2335646 (**2**), 2335647 (**3**), 2335648 (**4**), 2335649 (**5**), 2335650 (**6**), 2335651 (**7**), 2335652 (**8**), 2335653 (**9**), 2335654 (**11**) contain the supplementary crystallographic data for this paper. These data are provided free of charge by the joint Cambridge Crystallographic Data Centre and Fachinformationszentrum Karlsruhe.

## Acknowledgements

We thank Prof. Frank Breher and Prof. Peter Roesky for continuous support. Financial support by Deutsche Forschungsgemeinschaft (DFG) via the Emmy Noether Programme (HI 2063/1-1) and by Fonds der Chemischen Industrie via a Liebig Fellowship for M.P.M. is gratefully acknowledged. Ms. Helga Berberich is acknowledged for collecting NMR data. We acknowledge support by the state of Baden-Württemberg through bwHPC and DFG through grant no. INST 40/575-1 FUGG (JUSTUS 2 cluster). Open Access funding enabled and organized by Projekt DEAL.

## Conflict of Interest

The authors declare no conflict of interest.

## Data Availability Statement

The data that support the findings of this study are available in the supplementary material of this article.

**Keywords:** Acyclic Silylenes · Bonding · Low-Valent Main Group · Frontier Orbitals · Reactivity

- [1] P. Jutz, D. Kanne, C. Krüger, *Angew. Chem. Int. Ed.* **1986**, *25*, 164–164.
- [2] A. J. Arduengo, H. V. R. Dias, R. L. Harlow, M. Kline, *J. Am. Chem. Soc.* **1992**, *114*, 5530–5534.
- [3] M. Denk, R. Lennon, R. Hayashi, R. West, A. V. Belyakov, H. P. Verne, A. Haaland, M. Wagner, N. Metzler, *J. Am. Chem. Soc.* **1994**, *116*, 2691–2692.
- [4] M. Kira, S. Ishida, T. Iwamoto, C. Kabuto, *J. Am. Chem. Soc.* **1999**, *121*, 9722–9723.
- [5] M. Driess, S. Yao, M. Brym, C. van Wüllen, D. Lentz, *J. Am. Chem. Soc.* **2006**, *128*, 9628–9629.
- [6] M. Driess, S. Yao, M. Brym, C. van Wüllen, *Angew. Chem. Int. Ed.* **2006**, *45*, 6730–6733.
- [7] N. Takeda, H. Suzuki, N. Tokitoh, R. Okazaki, S. Nagase, *J. Am. Chem. Soc.* **1997**, *119*, 1456–1457.
- [8] N. Takeda, T. Kajiwara, H. Suzuki, R. Okazaki, N. Tokitoh, *Chem. Eur. J.* **2003**, *9*, 3530–3543.
- [9] R. S. Ghadwal, H. W. Roesky, S. Merkel, J. Henn, D. Stalke, *Angew. Chem. Int. Ed.* **2009**, *48*, 5683–5686.
- [10] A. C. Filippou, O. Chernov, G. Schnakenburg, *Angew. Chem. Int. Ed.* **2009**, *48*, 5687–5690.
- [11] R. S. Ghadwal, H. W. Roesky, C. Schulzke, M. Granitzka, *Organometallics* **2010**, *29*, 6329–6333.
- [12] R. S. Ghadwal, H. W. Roesky, K. Pröpper, B. Dittrich, S. Klein, G. Frenking, *Angew. Chem. Int. Ed.* **2011**, *50*, 5374–5378.
- [13] P. Ghana, M. I. Arz, G. Schnakenburg, M. Straßmann, A. C. Filippou, *Organometallics* **2018**, *37*, 772–780.
- [14] D. Geiß, M. I. Arz, M. Straßmann, G. Schnakenburg, A. C. Filippou, *Angew. Chem. Int. Ed.* **2015**, *54*, 2739–2744.
- [15] P. Ghana, M. I. Arz, U. Chakraborty, G. Schnakenburg, A. C. Filippou, *J. Am. Chem. Soc.* **2018**, *140*, 7187–7198.
- [16] C.-W. So, H. W. Roesky, J. Magull, R. B. Oswald, *Angew. Chem. Int. Ed.* **2006**, *45*, 3948–3950.
- [17] R. Rodriguez, D. Gau, Y. Contie, T. Kato, N. Saffon-Merceron, A. Baceiredo, *Angew. Chem. Int. Ed.* **2011**, *50*, 11492–11495.
- [18] I. Alvarado-Beltran, A. Baceiredo, N. Saffon-Merceron, V. Branchadell, T. Kato, *Angew. Chem. Int. Ed.* **2016**, *55*, 16141–16144.
- [19] S. Takahashi, J. Sekiguchi, A. Ishii, N. Nakata, *Angew. Chem. Int. Ed.* **2021**, *60*, 4055–4059.
- [20] B. D. Rekken, T. M. Brown, J. C. Fetting, H. M. Tuononen, P. P. Power, *J. Am. Chem. Soc.* **2012**, *134*, 6504–6507.
- [21] S. Inoue, K. Leszczyńska, *Angew. Chem. Int. Ed.* **2012**, *51*, 8589–8593.
- [22] A. V. Protchenko, K. H. Birjumar, D. Dange, A. D. Schwarz, D. Vidovic, C. Jones, N. Kaltsoyannis, P. Mountford, S. Aldridge, *J. Am. Chem. Soc.* **2012**, *134*, 6500–6503.
- [23] A. V. Protchenko, A. D. Schwarz, M. P. Blake, C. Jones, N. Kaltsoyannis, P. Mountford, S. Aldridge, *Angew. Chem. Int. Ed.* **2013**, *52*, 568–571.
- [24] D. Wendel, A. Porzelt, F. A. D. Herz, D. Sarkar, C. Jandl, S. Inoue, B. Rieger, *J. Am. Chem. Soc.* **2017**, *139*, 8134–8137.
- [25] T. Eisner, A. Kostenko, F. Hanusch, S. Inoue, *Chem. A Eur. J.* **2022**, *28*, e202202330.
- [26] D. Wendel, D. Reiter, A. Porzelt, P. J. Altmann, S. Inoue, B. Rieger, *J. Am. Chem. Soc.* **2017**, *139*, 17193–17198.
- [27] D. Reiter, P. Frisch, D. Wendel, F. M. Hörmann, S. Inoue, *Dalton Trans.* **2020**, *49*, 7060–7068.
- [28] D. Reiter, R. Holzner, A. Porzelt, P. J. Altmann, P. Frisch, S. Inoue, *J. Am. Chem. Soc.* **2019**, *141*, 13536–13546.
- [29] M. M. D. Roy, M. J. Ferguson, R. McDonald, Y. Zhou, E. Rivard, *Chem. Sci.* **2019**, *10*, 6476–6481.
- [30] M. M. D. Roy, S. R. Baird, E. Dornsiepen, L. A. Paul, L. Miao, M. J. Ferguson, Y. Zhou, I. Siewert, E. Rivard, *Chem. Eur. J.* **2021**, *27*, 8572–8579.
- [31] H. Zhu, A. Kostenko, D. Franz, F. Hanusch, S. Inoue, *J. Am. Chem. Soc.* **2023**, *145*, 1011–1021.
- [32] Y. K. Loh, L. Ying, M. Ángeles Fuentes, D. C. H. Do, S. Aldridge, *Angew. Chem. Int. Ed.* **2019**, *58*, 4847–4851.
- [33] A. Hinz, *Angew. Chem. Int. Ed.* **2020**, *59*, 19065–19069.
- [34] R. Guthardt, C. Jones, *Chem. Commun.* **2024**, 2022–2025.
- [35] Y. P. Zhou, S. Raoufoghaddam, T. Szilvási, M. Driess, *Angew. Chem. Int. Ed.* **2016**, *55*, 12868–12872.
- [36] X. Chen, H. Wang, S. Du, M. Driess, Z. Mo, *Angew. Chem. Int. Ed.* **2022**, *61*, e202114598.
- [37] R. Liu, Y. Tang, C. Wang, Z. F. Zhang, M. Der Su, Y. Li, *Inorg. Chem.* **2023**, *62*, 1095–1101.
- [38] M. Ghosh, S. Tothadi, S. Khan, *Organometallics* **2021**, *40*, 3201–3210.
- [39] R. Akhtar, S. H. Kaulage, M. P. Sangole, S. Tothadi, P. Parvathy, P. Parameswaran, K. Singh, S. Khan, *Inorg. Chem.* **2022**, *61*, 13330–13341.
- [40] M. Kaiser, M. P. Müller, F. Krätschmer, M. Rutschmann, A. Hinz, *Inorg. Chem. Front.* **2023**, *10*, 2987–2994.
- [41] M. P. Müller, A. Hinz, *Chem. Eur. J.* **2023**, *29*, e202302311.
- [42] R. A. Shaw, M. Woods, *J. Chem. Soc.* **1971**, 1569–1571.
- [43] G. Schott, B. Säverin, *Z. Chem.* **1968**, *8*, 428–429.
- [44] S. P. Green, C. Jones, A. Stasch, *Science* **2007**, *318*, 1754–1757.
- [45] P. Pykkö, M. Atsumi, *Chem. Eur. J.* **2009**, *15*, 12770–12779.
- [46] R. F. W. Bader, *Chem. Rev.* **1991**, *91*, 893–928.
- [47] T. Lu, F. Chen, *J. Comput. Chem.* **2012**, *33*, 580–592.
- [48] A. D. Becke, K. E. Edgecombe, *J. Chem. Phys.* **1990**, *92*, 5397–5403.
- [49] S. Shaik, D. Danovich, W. Wu, P. C. Hiberty, *Nat. Chem.* **2009**, *1*, 443–449.
- [50] S. Shaik, D. Danovich, J. M. Galbraith, B. Braïda, W. Wu, P. C. Hiberty, *Angew. Chem. Int. Ed.* **2020**, *59*, 984–1001.
- [51] I. Alvarado-Beltran, A. Rosas-Sánchez, A. Baceiredo, N. Saffon-Merceron, V. Branchadell, T. Kato, *Angew. Chem. Int. Ed.* **2017**, *56*, 10481–10485.
- [52] T. Iwamoto, H. Masuda, S. Ishida, C. Kabuto, M. Kira, *J. Am. Chem. Soc.* **2003**, *125*, 9300–9301.
- [53] R. Kobayashi, S. Ishida, T. Iwamoto, *Angew. Chem. Int. Ed.* **2019**, *58*, 9425–9428.
- [54] P. Hädinger, M. P. Müller, A. Hinz, *Inorg. Chem.* **2024**, *63*, 1997–2004.
- [55] J. Niesmann, U. Klingebiel, M. Schäfer, R. Boese, *Organometallics* **1998**, *17*, 947–953.
- [56] P. P. Samuel, R. Azhakar, R. S. Ghadwal, S. S. Sen, H. W. Roesky, M. Granitzka, J. Matussek, R. Herbst-Irmer, D. Stalke, *Inorg. Chem.* **2012**, *51*, 11049–11054.
- [57] A. Hinz, *Chem. Eur. J.* **2019**, *25*, 3267–3271.
- [58] M. Cheng, D. R. Moore, J. J. Reczek, B. M. Chamberlain, E. B. Lobkovsky, G. W. Coates, *J. Am. Chem. Soc.* **2001**, *123*, 8738–8749.
- [59] J. E. Borger, A. W. Ehlers, M. Lutz, J. C. Slootweg, K. Lammertsma, *Angew. Chem.* **2014**, *126*, 13050–13053.
- [60] G. M. Sheldrick, *Acta Crystallogr. Sect. A* **2015**, *71*, 3–8.
- [61] G. M. Sheldrick, *Acta Crystallogr. Sect. A* **2008**, *64*, 112–122.
- [62] C. B. Hübschle, G. M. Sheldrick, B. Dittrich, *J. Appl. Crystallogr.* **2011**, *44*, 1281–1284.

- [63] M. J. Frisch, G. W. Trucks, H. B. Schlegel, G. E. Scuseria, M. A. Robb, J. R. Cheeseman, G. Scalmani, V. Barone, G. A. Petersson, H. Nakatsuji, X. Li, M. Caricato, A. V. Marenich, J. Bloino, B. G. Janesko, R. Gomperts, B. Mennucci, H. P. Hratchian, J. V. Ortiz, A. F. Izmaylov, J. L. Sonnenberg, D. Williams-Young, F. Ding, F. Lipparini, F. Egidi, J. Goings, B. Peng, A. Petrone, T. Henderson, D. Ranasinghe, V. G. Zakrzewski, J. Gao, N. Rega, G. Zheng, W. Liang, M. Hada, M. Ehara, K. Toyota, R. Fukuda, J. Hasegawa, M. Ishida, T. Nakajima, Y. Honda, O. Kitao, H. Nakai, T. Vreven, K. Throssell, J. A. J. Montgomery, J. E. Peralta, F. Ogliaro, M. J. Bearpark, J. J. Heyd, E. N. Brothers, K. N. Kudin, V. N. Staroverov, T. A. Keith, R. Kobayashi, J. Normand, K. Raghavachari, A. P. Rendell, J. C. Burant, S. S. Iyengar, J. Tomasi, M. Cossi, J. M. Millam, M. Klene, C. Adamo, R. Cammi, J. W. Ochterski, R. L. Martin, K. Morokuma, O. Farkas, J. B. Foresman, D. J. Fox, Gaussian 16, Revision B.01, Gaussian Inc. Wallingford CT, **2016**.
- [64] E. D. Glendening, C. R. Landis, F. Weinhold, *J. Comput. Chem.* **2013**, *34*, 1429–1437.
- [65] R. K. Harris, E. D. Becker, S. M. C. De Menezes, R. Goodfellow, P. Granger, *Solid State Nucl. Magn. Reson.* **2002**, *22*, 458–483.
- [66] G. R. Fulmer, A. J. M. Miller, N. H. Sherden, H. E. Gottlieb, A. Nudelman, B. M. Stoltz, J. E. Bercaw, K. I. Goldberg, *Organometallics* **2010**, *29*, 2176–2179.
- [67] S. J. McLain, J. C. Calabrese, J. Feldman, A. Parthasarathy, W. J. Marshall, S. D. Arthur, *Organometallics* **2002**, *16*, 1514–1516.
- [68] S. J. Bonyhady, C. Jones, S. Nembenna, A. Stasch, A. J. Edwards, G. J. McIntyre, *Chem. Eur. J.* **2010**, *16*, 938–955.
- [69] J. Hicks, M. Juckel, A. Paparo, D. Dange, C. Jones, *Organometallics* **2018**, *37*, 4810–4813.
- [70] P. P. Power, *Inorganic Synthesis*, John Wiley & Sons, **2018**.
- [71] N. C. Bruno, M. T. Tudge, S. L. Buchwald, *Chem. Sci.* **2013**, *4*, 916–920.
- [72] R. García-Rodríguez, H. Liu, *Chem. Commun.* **2013**, *49*, 7857–7859.
- [73] L. P. Spencer, P. Yang, B. L. Scott, E. R. Batista, J. M. Boncella, *Inorg. Chem.* **2009**, *48*, 2693–2700.
- [74] J. Gavenonis, T. D. Tilley, *Organometallics* **2002**, *21*, 5549–5563.

Manuscript received: March 18, 2024

Accepted manuscript online: April 24, 2024

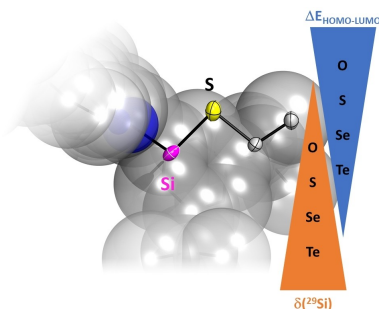
Version of record online: ■■■, ■■■

## Research Articles

## Low-Valent Compounds

M. P. Müller, A. Hinz\* — e202405319

Silylenes with a Small Chalcogenide Substituent: Tuning Frontier Orbital Energies from O to Te



Acyclic dicoordinated silylenes with small chalcogenide substituents were prepared and characterised, enabled by a bulky carbazolyl scaffold. The electronic properties change dramatically from O to Te, with decreasing HOMO–LUMO gaps and increasing chemical shift of the  $^{29}\text{Si}$  NMR resonances.